

State Transition Based Behavioural Model for Electric Arcs in 48 V Automotive Power Supply Networks

Carina Austermann, Michael Kiffmeier, Stephan Frei
On-board Systems Lab
TU Dortmund University
Dortmund, Germany
carina.austermann@tu-dortmund.de

Abstract — The possibility of arc faults exists in various technical applications. Hence, arcing has been the subject of many investigations up until today. The upcoming 48 V voltage level creates the necessity to consider the arc event in the automotive environment. In general, an arc can occur anywhere in the wire harness, either as series or parallel arc. The large amount of dissipated power, resulting in extremely high temperatures, leads to the risk of fire. In order to understand the generation of arcs and the conditions needed to extinguish the arc, automotive supply networks simulation is beneficial. Accurate models for the supply components and the arc are required. This paper presents a DC arc behavioural model for network simulations in a 48 V automotive supply system. The arc voltage is modelled by a current controlled voltage source with a complex function with constant parameters. With the help of a state transition diagram, short circuits and open contacts are considered, as well. The model is evaluated in different circuit setups and it is verified by measurements.

Keywords—DC arc model, 48 V automotive supply system

I. INTRODUCTION

The 48 V voltage level has been introduced in vehicles to meet the higher power demands caused by modern power electronic systems. While in 12 V and 24 V systems the risk of electric arcs was extremely low, in 48 V systems an electric arc must be taken into account as critical fault. The high power dissipated in an arc can lead to dangerous damages up to vehicle fire. Understanding the electric behaviour of the arc in the vehicle supply network is an important requirement in order to estimate the risk in vehicles. The model-based investigation of power supply systems is an important step in the current design processes. Arc risk analysis can be integrated in this investigation, when appropriate arc models are available.

Modelling the electric arc has been already the subject of numerous investigations. Three different types of models can be found: physical models, black box models and parametric models [1]. Whereas physical models consider the intrinsic plasma physical processes and parametric models are based on graphics and diagrams, in this paper an available behavioural model is extended and parameterised. The model can be used in

many network simulation tools and the transient behaviour as well as the dissipated energy of the arc can be calculated.

Many published behavioural model approaches are based on the models of Cassie [2] and Mayr [3]. These models describe the arc dynamics with a differential equation for the arc conductivity and were adapted in several ways [4]. These models are often used in AC circuit simulations [4], [5]. There are some investigations on the use of these models in DC networks [6]. It was found that also the application in DC networks is possible, but there are some restrictions concerning the voltage and current ranges and the estimation of dynamic parameters is complex. Another way of model generation is a quasi-static approach based on the V - I -characteristic. The static behaviour can be described by the use of an algebraic equation with constant parameters. The first static equation was published by Ayrton [7]. Many adaptations of these equations are presented and used in several applications, e.g. [8]-[10]. This model approach is the basis of the presented arc model in this paper.

The paper is organized as follows. Chapter II includes the description of the model structure and the implementation. Chapter III presents measurement results, which are used to parameterise the model. The parameterised model is verified by measurements in Chapter IV with different network setups to demonstrate the model accuracy.

II. ARC MODEL

In this chapter, a state transition based behavioural model for DC arcs is described and an example implementation in Matlab Simulink/Simscape, to simplify the useful addition to already existing equivalent circuit representations of power supply systems, is presented. A mathematical description for the relation between the arc voltage, current and its length is suggested and discussed.

A. Model Structure

The arc is modelled as a two pole circuit network element with several case distinctions. The value of the gap distance $d(t)$ is an independent input parameter. The model structure, shown in Figure 1, can be divided into two parts: circuit layer and circuit control layer. The circuit layer consists of an equivalent circuit

with the components: controlled voltage source v_{arc} , variable resistance R_{gap} and a current measurement. The variable resistance describes the behaviour of the gap before the ignition and after the expiration of the arc event, or short- and open-circuit situations. This general approach of using a controlled voltage source, representing the characteristic arc voltage, and a variable resistance was already presented in previous publications [11], [12]. The controlled voltage source models the voltage drop of the burning arc, depending on the gap distance d and the arc current i_{arc} .

The control layer contains a state transition model and the arc function for the current controlled voltage source. The state transition model consists of the three states: short-circuit, open-circuit and arc. Each transition is triggered by certain conditions. The two parts of the control layer are described in detail in the following sections.

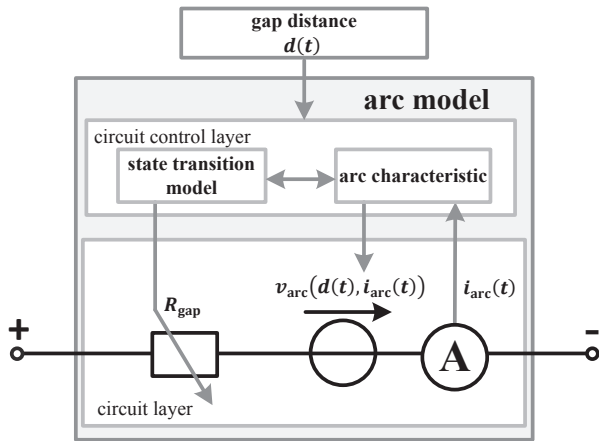


Figure 1: Block diagram of the model structure

B. State Transition Model

The arc fault behaviour can be represented by a state transition diagram (Figure 2). There are three different electrical states of an arc fault: short circuit, open circuit and the arc itself. The model includes different transitions between the states to simulate an arc event over the course of time. The simulation can start in the short circuit or the open circuit state. The electric behaviour of the initial state is modelled with the variable resistance R_{gap} . The transition from short circuit state to open circuit state describes the circuit opening without arcing. If the current does not exceed the minimum arc current, a stable arc cannot exist [13].

It is only possible to reach the arc state proceeding from the short circuit state when there is a gap distance. In the considered voltage range an avalanche breakdown can only occur with a small contact gap of $d < 30 \mu\text{m}$ and depends on the conditions of the electrodes [13]. This arcing process can be seen as an exception and is neglected in the presented model approach.

The transition between the short circuit state and the arc state, models the ignition process of an arc. To sustain a stable arc the available voltage must be higher than the minimum arc voltage and the current must be larger than the minimum arc current i_{min} . These values for a stable arc mainly depend on the electrode material [13]. According to this, the requirements of an arc

ignition are $d > 0$ and $i > i_{\text{min}}$. Because of the implementation with a voltage source the voltage condition has to be neglected. In the arc state the controlled voltage source models the arc voltage drop based on the arc current and the gap distance. The arc state is kept until the arc current becomes zero or the electrodes are connected again. When the arc is expired, caused by a current drop, the open circuit state is achieved. The open circuit state is represented with a high-resistance state of the arc gap. In this state, the voltage source has the value of zero and the resistive characteristic is modelled with an increasing R_{gap} . To prevent a discontinuous waveform at the extinction moment, R_{gap} must start with the value of $v_{\text{arc}}/i_{\text{arc}}$ in the moment of expiration. R_{gap} increases with a high slope and the voltage drop of the gap reaches the maximum available voltage.

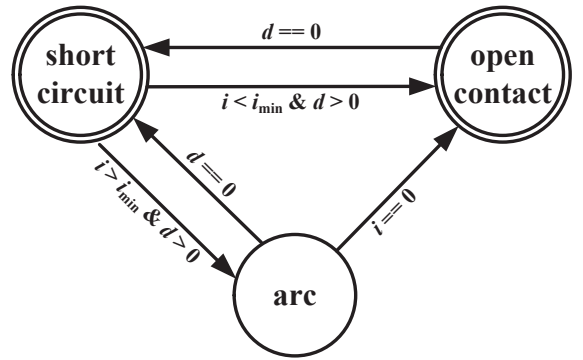


Figure 2: State transition diagram

C. Arc Characteristic

The arc equation published by Ayrton describes the static V - I -characteristic of an arc [7]. The equation is given in (1) and describes the arc voltage v_{arc} as a function of the arc current i_{arc} and the arc length d . It consists of a constant term that describes the characteristic voltage step which is part of the ignition process. The linear term describes the increase of the voltage across the arc column. The third term describes the non-linear behaviour of the V - I -characteristic.

$$v_{\text{arc}}(i_{\text{arc}}, d) = A + B \cdot d + \frac{C+D \cdot d}{i_{\text{arc}}} \quad (1)$$

This equation was used for different static and quasi-static simulations with acceptable results (e.g. [14]). In many cases it is impossible to find a constant parameter set suitable for a large range of voltages and currents. Some approaches try to solve this problem with a continuous adaption of the parameters (e.g. [15]) but this causes a complex implementation.

In Figure 3 the qualitative relation between the arc voltage and the contact gap length is shown [16]. It can be seen that there is a non-linear relation between d and v_{arc} in the range of short distances. The nonlinearity is characterized by a decreasing slope with an increasing contact gap. Furthermore, the voltage is weakly current-dependent in this range. An explanation for this nonlinearity, mentioned in [16], is the decreasing quotient between the axial heat conduction and the overall heat conduction with increasing contact gap. For this reason, there is a linear relation between voltage and distance in the range of

longer arcs. The Ayrton equation is based on this linear relation, which is shown in an exemplary way in Figure 3. In a 48 V automotive supply system the operating voltage is up to 60 V and possible arc lengths are up to 30 mm [16]. The range of validity in automotive applications is shown in Figure 3 and reveals that a linear approach is not sufficient. The automotive environment necessitates an adaption of equation (1) to allow a quantitative simulation.

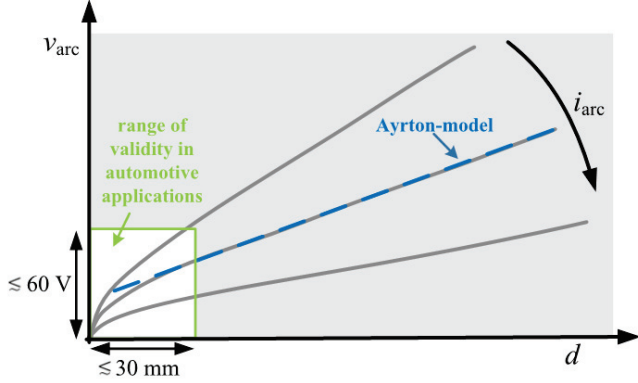


Figure 3: Applicability of the different arc models, measurement results of a free-burning arc in air [16]

Figure 4 shows measurement results of the arc voltage as a function of the contact gap for three different arc currents in a 48 V supply system. The non-linear relation between voltage and gap length can be seen. This measurement verifies the qualitative relation shown in Figure 3 and can be used to find a new function to describe the arc characteristic.

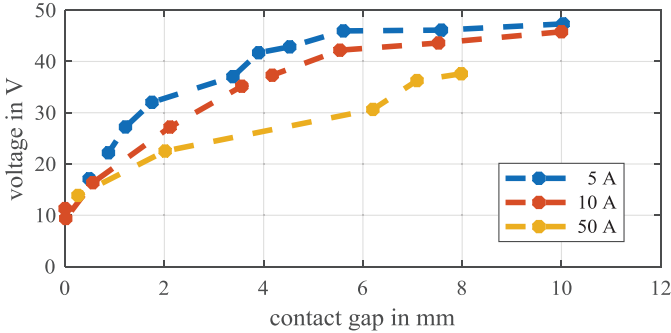


Figure 4: Measurement results of the arc voltage over gap length

Equation (1) was modified in order to consider accurately short gap lengths (2). The modified function consists of three terms with four constant parameters. The constant term describes the ignition voltage which depends on the cathode and anode voltage drop [16]. The \ln -term is used to describe the non-linear relation between the voltage and the contact gap. This term is the significant difference to (1) and is derived from Figure 3 and 4. The term which includes the arc current describes the non-linear behaviour. To illustrate this behaviour, the arc can be seen as a variable circular conductor. An increasing current flow leads to a greater cross section of the arc column which decreases the voltage drop.

$$v_{\text{arc}}(i_{\text{arc}}, d) = A + B \cdot \ln(C \cdot d + 1) + \frac{D \cdot d}{i_{\text{arc}}} \quad (2)$$

The graphical representation of this equation is shown in Figure 5. The V - I -characteristics are given for some exemplary gap lengths. The enlargement of the gap length leads to a nonlinear decreasing distance between the V - I -characteristic curves.

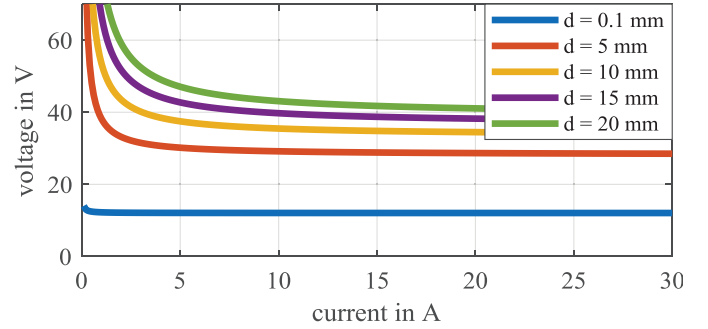


Figure 5: V - I -characteristics created with the presented arc equation (2)

III. PARAMETERIZATION MEASUREMENTS

In this section, arc-investigations with a measurement setup are presented. The measurement results are used to build a data base to parameterise the arc equation (2). The measured arcs are also used to validate the simulation model.

A. Measurement Setup

The used measurement environment for arc faults consists of a power supply, a resistive load and a motor driven contact separation unit to initiate the arc. The simplified circuit diagram of the measurement setup is shown in Figure 6. The resistive load is varied to measure arcs with different maximum currents. The motor driven contact separation unit consists of a linear drive with stepper motor, typical automotive plug-in contacts and a microcontroller based control unit. The setup can be seen in Figure 7. The plug-in contacts consist of silver-plated copper alloy. In the presented measurements a contact profile with a constant separating velocity is chosen.

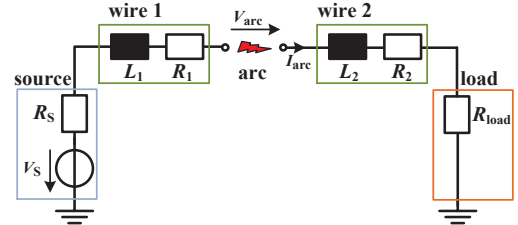


Figure 6: Equivalent circuit diagram of the measurement setup

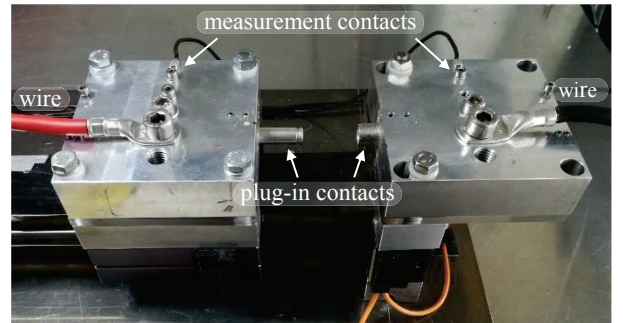


Figure 7: Contact separation unit with automotive plug-in contacts

B. Measurement results

A typical voltage and current waveform of a series arc in a resistive network ($R_{\text{load}} = 0.3 \Omega$) is shown in Figure 8. The arc electrodes are separated with a constant speed of $188 \text{ mm}\cdot\text{s}^{-1}$. In this waveform the typical steep voltage step of the arc ignition is visible ($t = 20 \text{ ms}$). The ignition voltage reaches the value of 13 V . The nonlinear behaviour of the arc by constant contact opening is shown. The arc reaches a maximum length of $d = 18 \text{ mm}$. The arc length is a characteristic value because it has a great influence on the arc energy and it has to be quantitatively considered in the simulation.

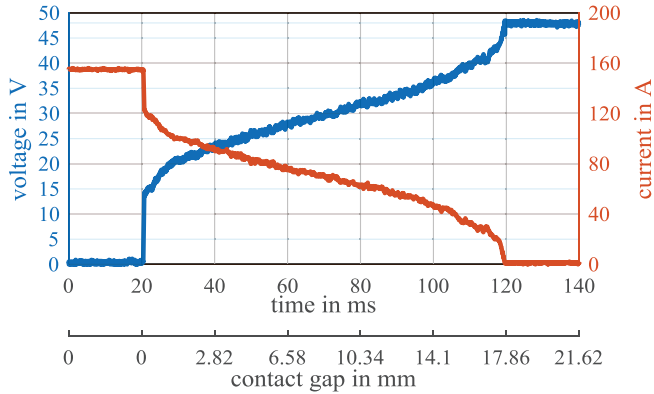


Figure 8: Voltage and current waveform of a series arc in a setup with $V_s = 48 \text{ V}$, $R_{\text{load}} = 0.3 \Omega$ and $v = 188 \text{ mm}\cdot\text{s}^{-1}$

In Figure 9 a set of resistive measurements is shown. One measured arc leads to different operating points, which can be seen as one line in the figure. A small resistive load R_{load} leads to an increased arc current as well as an increased maximum arc length. The voltage characteristic can be seen in the colour gradient.

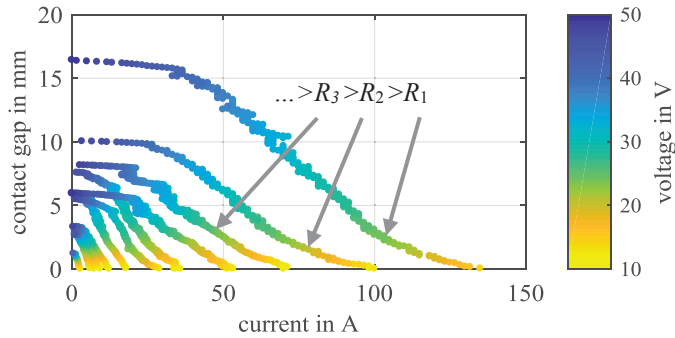


Figure 9: Measurement results of arc current and voltage in different resistive networks

C. Parameterisation

A curve fitting based on the least square method is used to find from Figure 8 a parameter set for the arc equation (2). The extracted parameter set is presented in table 1.

TABLE 1: ARC EQUATION PARAMETER

PARAMETER	VALUE
A	11 V
B	8.52 V
C	1.3 mm^{-1}
D	$2 \text{ VA}\cdot\text{mm}^{-1}$

A graphical representation of the fitting results is shown in Figure 10 using a colour gradient. In this figure the relative deviation r_v between the measured and the calculated arc voltages can be seen. The used formula for the relative deviation is given in (3). The results show a good agreement between the measured and computed arc voltage. In the range of small currents the deviation decrease, because of statistic variation in the arc length. The accuracy of the results increase with increasing arc current. These configurations lead to higher arc energies and are the important scenarios for the risk evaluation in automotive supply systems.

$$r_v = \text{abs} \left(\frac{v_{\text{model}} - v_{\text{meas}}}{v_{\text{meas}}} \right) \cdot 100\% \quad (3)$$

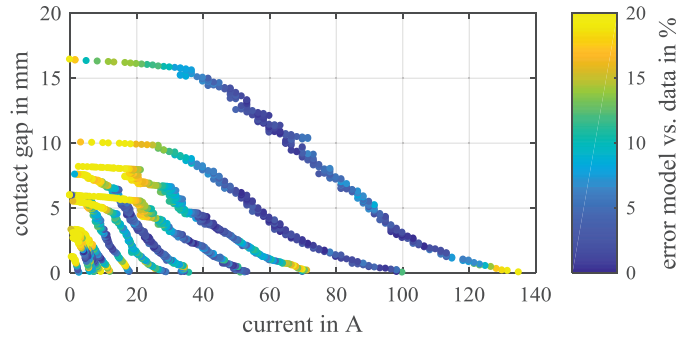


Figure 10: Relative error of modelling results for the arc voltage in comparison to the measurement results

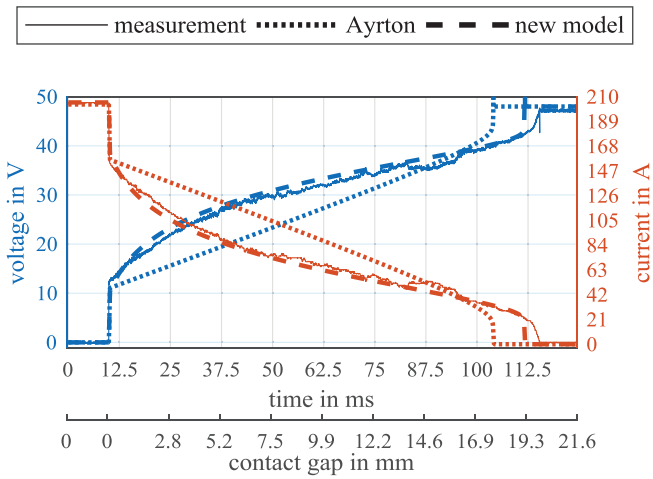
IV. MODEL VALIDATION

In this chapter, time domain simulations with the developed arc model are presented and compared to measurements. The applicability for different setups, varying arc currents and voltages is shown.

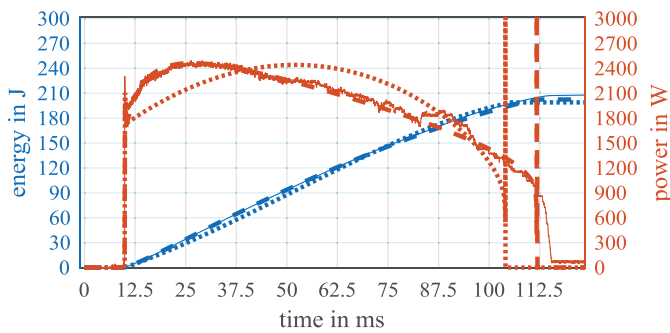
A. Verification in resistive networks

A comparison between simulation results computed by the new developed model and the Ayrton model, as well as a measured waveform is shown in Figure 11. The used setup has a resistive load $R_{\text{load}} = 0.22 \Omega$ and a source voltage of $V_s = 48 \text{ V}$. The electrodes are separated with a constant velocity of $v = 188 \text{ mm}\cdot\text{s}^{-1}$. It can be seen, that the Ayrton model is not able to emulate the correct voltage and current waveforms. In Figure 11 (b) the power and energy of the arc is shown. The simulated arc energy is very close to the measured energy.

The arc energy is an important value because it describes the potential risk of an arc event. In Figure 12 the comparison between measured and simulated dissipated energy values for varying load resistances is shown. The simulation results match the measured energy values very well.



(a)



(b)

Figure 11: Comparison between measured and simulated waveform for a resistive network setup with $V_S = 48 \text{ V}$, $R_{\text{load}} = 0.23 \Omega$ and $v = 188 \text{ mm}\cdot\text{s}^{-1}$

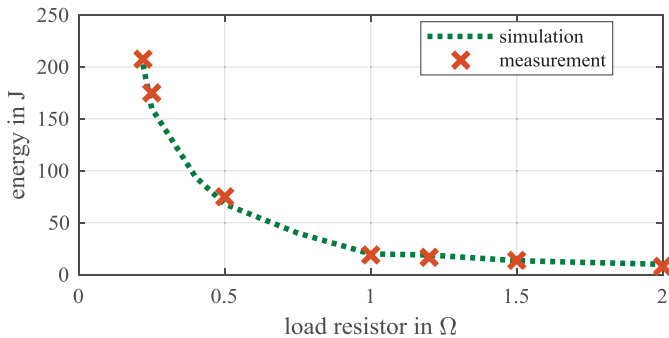


Figure 12: Comparison between measured and simulated arc energies in different resistive network setups with a constant separating velocity of $v = 188 \text{ mm}\cdot\text{s}^{-1}$

B. Verification of the voltage range in resistive networks

The previous measurements use a voltage level of 48 V. It is important, that the model can be used up to 60 V as temporarily permitted maximum voltage. In the Figure 13 and Figure 14 comparisons between measured and simulated arc values are shown, to verify the model further. Source voltages of 30 V and 60 V in resistive networks are used. It can be seen, that the maximum voltage has a great influence on the arc length and the

dissipated arc energy. The arc model delivers good results for both voltage levels.

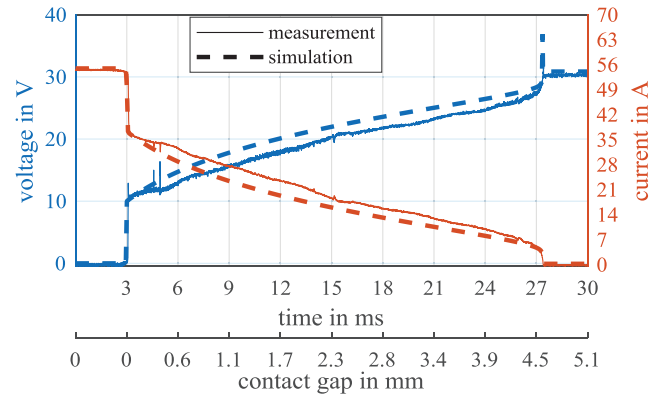


Figure 13: Comparison between measured and simulated waveform for a resistive network setup with $V_S = 30 \text{ V}$, $R_{\text{load}} = 0.54 \Omega$ and $v = 188 \text{ mm}\cdot\text{s}^{-1}$

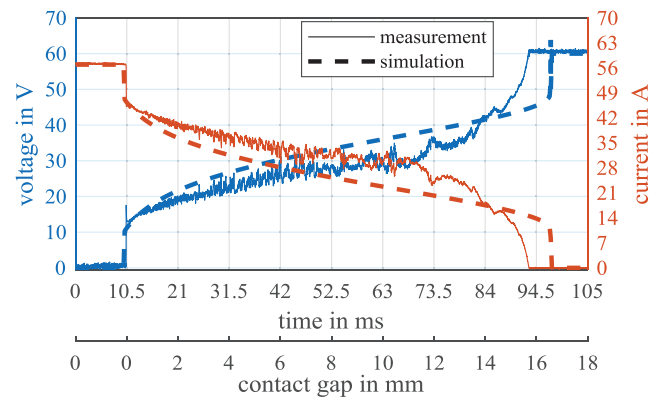


Figure 14: Comparison between measured and simulated waveform for a resistive network setup with $V_S = 60 \text{ V}$, $R_{\text{load}} = 1 \Omega$ and $v = 188 \text{ mm}\cdot\text{s}^{-1}$

C. Transient behaviour in the arc ignition phase

A more realistic load configuration is a parallel capacitive-resistive load, e.g. for voltage stabilisation within the electronic control units. The wire inductance and the load capacitance create an oscillatory circuit. The steep voltage step in the moment of the arc ignition leads to an oscillation in the arc current. This oscillation has a great influence on the arc behaviour. As soon as the oscillation reduces the arc current to zero the arc expires.

Two possible waveforms caused by an oscillation in the arc current are shown in the following Figure 15. Figure 15 (a) shows an arc that is influenced by an oscillation. The arc current drops down to 5 A but after the transient effect the arc reaches stable operating points. The arc energy is the same as in the setup with a purely ohmic load. An arc interruption in the ignition moment is shown in Figure 15 (b). The arc sustains for 50 μs before the arc expires and the capacitor characteristic can be seen. This fast expiration leads to a small arc energy and reduces the potential risk of an arc fault. The transient measurements validate the developed arc model further. In the Figure 15 the simulated results (dashed lines) are compared with the measurement results. In both cases the model emulates the arc voltage and current properly. The model shows the correct behaviour in the case of an oscillating arc current. The special

case of an arc interruption in the ignition can also be simulated with the presented model.

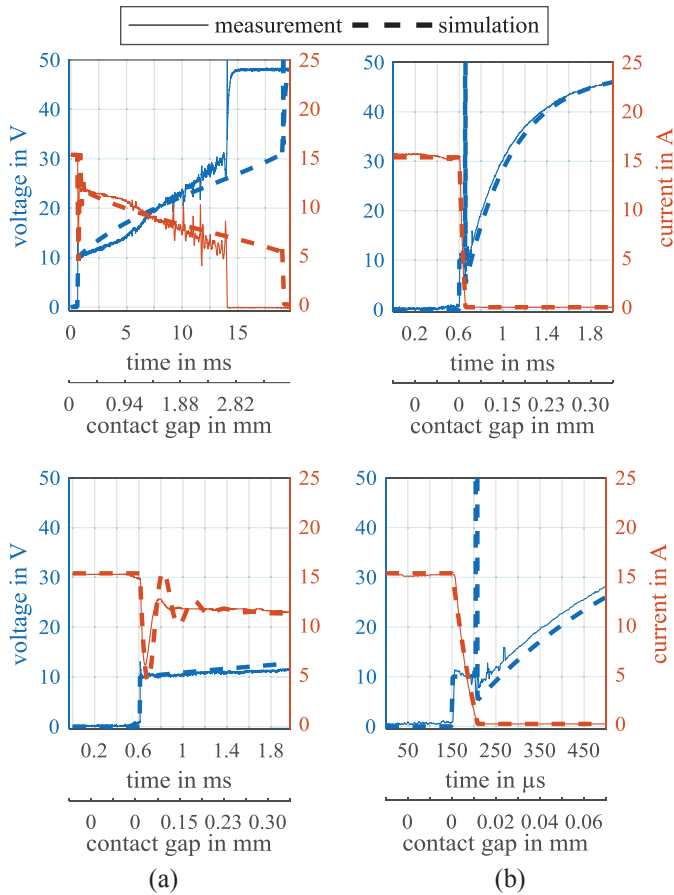


Figure 15: Comparison between measured and simulated waveforms for two different setups $R_{load} = 3 \Omega$, $L_2 = 33 \mu\text{H}$, $ESR = 150 \text{ m}\Omega$ and (a) $C_{load} = 47 \mu\text{F}$, (b) $C_{load} = 147 \mu\text{F}$

V. CONCLUSION

In this paper, the arc event in an automotive environment has been analysed and modelled. A state transition based behavioural model is presented. A new arc equation for the quasi-static arc characteristic has been developed to meet the requirements in 48 V automotive power supply systems. The developed model was parameterised, based on measurements and validated in different network setups. The simulation model delivers static and dynamic voltages, currents and energy that are

very close to measurements, so that the model is suitable for network simulations.

REFERENCES

- [1] L. van der Sluis and W.R. Rutgrs, "Comparison of Test circuits for High Voltage Circuit Breakers by Numerical Calculations with Arc Models," *IEEE Transactions on Power Delivery*, vol. 7, no. 4, Oct. 1992
- [2] A.M. Cassie, "Theorie nouvelle des arcs de rupture et de la rigidite des circuits," *CIGRE Report*, 1939
- [3] O. Mayr, "Beiträge zur Theorie des statischen und des dynamischen Lichtogens," *Archiv für Elektrotechnik*, vol. Band 37, Heft 12, pp 588-608
- [4] A. Parizad, H. R. Baghaee, A. Tavakoli and S. Jamali, "Optimization of Arc Models Parameters Using Genetic Algorithm", *IEEE International Conference on Electric Power and Energy Conversion Systems*, 2010
- [5] J. Andrea, P. Besdel, O. Zim und M. Bourmat, "The Electrical Arc as a Circuit Component", *IECON 2015-41st Annual Conference of the IEEE*, 2015
- [6] K.-H. Park, H.-Y. Lee, T.-Y. Shin and C.-W. Gu, "Assessment of Various Kinds of AC Black-Box Arc Models for DC Circuit Breaker", *4th International Conference on Electric Power Equipment – Switching Technology*, 2017
- [7] H. Ayrton, *The Electric Arc*, London: The Electrician, 1902.
- [8] C. P. Steinmetz, "Transformation of electric power into light," *American Institute of Electrical Engineers*, New York, 1906.
- [9] W. B. Nottingham, "A New Equation for the Static Characteristic of the Normal Electric Arc," *American Institute of Electrical Engineers*, New York, 1925
- [10] R. F. Ammermann, T. Gammon, P .K. Sen and J. P. Nelson, "DC-Arc Models and Incident-Energy Calculations," *IEEE Transactions on Industry Applications*, vol. 46, no. 5, Sept./Oct. 2010
- [11] F. M. Uriate, A. L. Gattozzi, J. D. Herbst, H. B. Estes, T.J. Hotz, A. Kwasinski and R.E. Hebner, "A DC Arc Model for series faults in Low Voltage Microgrids," *IEEE Transactions on Smart Grid*, vol. 3, no. 4, Dec. 2012
- [12] F. M. Uriate, H. B. Estes, T. J. Hotz, A. L. Gattozzi, J. D. Herbst, A. Kwasinski and R. E. Hebner "Development of a Series Fault Model for DC Microgrids," *IEEE PES Innovative Smart Grid Technologies*, 2011
- [13] P. Slade, *Electrical Contacts-Principles and Applications*, Boca Raton: Taylor&Francis Group, LLC, 2014
- [14] M. Kiffmeier, S. Önal, C. Austermann and S. Frei, "Modelling of Arc Faults in 48 V Automotive Power Supply Systems," *IEEE Vehicle Power and Propulsion Conference*, 2017
- [15] M. Buffo, J.-P. Martin, S. Saadate, J. Andrea, N. Dumoulin and E. Guillard, "Study of the Electric Arc in DC Contactors: Modeling, Simulation and Experimental Validation," *IEEE Holm Conference on Electrical Contacts*, 2017
- [16] W. Rieder, *Plasma und Lichtbogen*, Braunschweig: Friedr. Vieweg & Sohn GmbH, 1967
- [17] Y.-J. Kim and H. Kim, "Modeling for series arc of DC circuit breaker," *6th International Conference on Renewable Energy Research and Applications*, 2017